

Measurement of the ferromagnetic relaxation in a micron-size sample

O. Klein,^{1,*} V. Charbois,¹ V. V. Naletov,^{1,2} and C. Fermon¹

¹*Service de Physique de l'État Condensé, CEA Orme des Merisiers, F-91191 Gif-Sur-Yvette, France*

²*Physics Department, Kazan State University, Kazan 420008, Russia*

(Received 14 March 2003; published 27 June 2003)

It is shown that magnetic-resonance force microscopy can provide direct measurements of both the longitudinal and the transverse relaxation rates in a micron-size ferromagnetic sample. As a demonstration, we have applied the technique to a single crystal disk of yttrium iron garnet. Separation between the individual relaxation channels is achieved through a comparison of the results obtained by three different experiments: resonance linewidth measurements, source and frequency modulation, and quantitative measurement of the longitudinal magnetization.

DOI: 10.1103/PhysRevB.67.220407

PACS number(s): 76.50.+g, 07.79.Pk, 07.55.-w

One of the main applications of ferromagnetic resonance spectroscopy is to measure the dissipative term that enters in the equation of motion for the magnetization vector. The processes, whereby the total magnetization M approaches equilibrium, reveal the coupling between the spin system and the other degrees of freedom. In a spin ordered state, the spatial fluctuations of the motion (spin waves), rather than the thermal fluctuations, are the disturbances that may alter the experimentally determined value of the relaxation rate. At the microscopic scale (dimensions smaller than the exchange length), the norm of $|M|$ is a constant of the motion and the dissipative term takes the phenomenological Gilbert form.^{1,2} At the macroscopic scale, however, the conditions that determine the decay of the spatially averaged \bar{M} may be less strict. Spatial decoherence of the motion may lead to an apparent faster decay rate of the transverse component depending on the structural inhomogeneities (defects, surface roughness, etc), while the longitudinal component M_z (the z axis is defined along the precession axis) always approaches equilibrium at the intrinsic spin thermalization rate $1/T_1$. Different transverse and longitudinal relaxation times are accounted by the Bloembergen's equations of motion,³ a form which is reminiscent of the Bloch's equations used in paramagnetic resonance. In contrast to paramagnets, the longitudinal relaxation time T_1 of ferromagnets cannot be measured by either a standard pulsed decay scheme or a saturation experiment (a measurement of $h_{\text{sat}}^2 = 1/\{\gamma^2 T_1 T_2\}$), because a premature "sticking" of the transverse magnetization occurs beyond the so-called Suhl threshold.⁴ A direct determination of T_1 requires an accurate measurement of the change of M_z in the small motion limit.⁵ This was achieved 50 years ago by Bloembergen and Wang⁶ and later by Flechter *et al.*⁷ using a z -direct pickup coil. The approach, however, lacks the sensitivity of a standard susceptibility measurement because $M_z \propto \cos \theta$ is a second order effect in the canting angle θ . Therefore, it cannot be applied onto lithographically patterned thin films that compose modern spin electronic devices.

In this paper, we propose to use ferromagnetic resonance force microscopy (fMRFM) to measure the intrinsic ferromagnetic relaxation rates inside a micron-size sample. In a recent paper,⁸ it was shown that mechanical detection affords

a very sensitive means of measuring quantitative changes in \bar{M}_z , produced when the sample absorbs energy from the high-frequency (hf) field. We will present our results obtained at room temperature on a test sample of yttrium iron garnet (YIG). The sample is a disk⁹ of diameter $D = 160 \mu\text{m}$ and thickness $S = 4.75 \mu\text{m}$ perpendicularly magnetized in a static field H_{ext} of a few kilooersted and excited by microwave fields between 5 and 13.5 GHz. The distance between the sample and the probe is fixed at $\ell = 100 \mu\text{m}$ so that their coupling is in the weak-interaction regime.¹⁰ The spatial average of the transverse component of the magnetization \bar{M}_t is measured independently by a standard setup (see Fig. 1). The power reflected off a half-wavelength resonator is detected by a microwave crystal diode, carefully calibrated so that the signal is square law over the measured range. The diode signal is then proportional to the microwave power absorbed, $P_{\text{abs}} \propto \chi''$, the imaginary part of the microwave susceptibility. For a magnetization that follows the Bloch's equation of movement, this quantity varies with H_{ext} in the same manner as \bar{M}_t^2 .

In ferromagnetic resonance (FMR) studies, the conventional way of evaluating the damping coefficient is to measure the width of the absorption line at low incident power ($P_{\text{in}} = 5 \mu\text{W}$ in our case). The shape of the resonance is obtained by scanning the magnetic field H_{ext} through the region of resonance when the microwave frequency is maintained constant at the eigenfrequency of an almost critically coupled microstrip resonator ($f_0 = 10.47 \text{ GHz}$). For \bar{M}_z , a substantial gain in sensitivity can be achieved by modulating the magnetization at the fundamental flexure mode of the cantilever, ω_c . In this section, we use source modulation, which corresponds to a modulation in amplitude of the incident microwave, $H_1 \{1 + (\epsilon/2) \cos(\omega_s t) - (\epsilon/2)\} \hat{x}$, with ω_s the modulation frequency, H_1 the circularly polarized amplitude of the microwave field, and ϵ the fraction of modulation. This approach is best suited for low-power studies (much below the Suhl threshold), as one can take advantage of the full amplitude ($\epsilon = 1$) without inducing line-shape distortion. Figure 2(a) displays the measurement of both $M_s - \bar{M}_z$ (M_s is the saturation magnetization at the temperature of the experiment) and \bar{M}_t^2 as a function of H_{ext} on a semilogarithmic

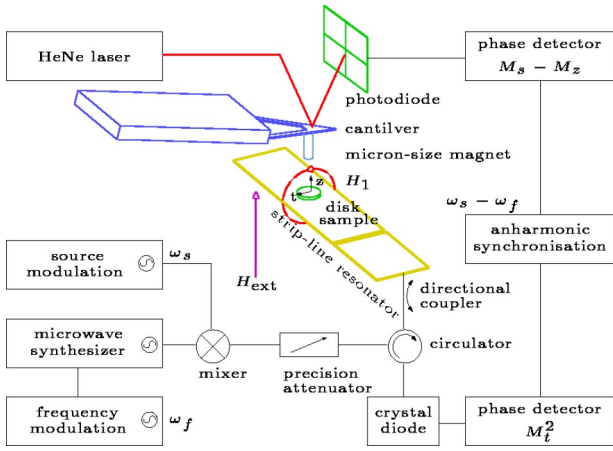


FIG. 1. Block diagram of the experimental apparatus, which measures both $M_s - \bar{M}_z$ and \bar{M}_t^2 simultaneously.

scale. We observe an intense resonance peak at 5324.5 Oe, the fundamental mode, and all the higher harmonics⁹ are outside the figure range. It can be seen in Fig. 2(a) that the main resonance is followed by a series of two weaker peaks located on its low-field wing and ≈ 3 Oe apart. These weaker modes get stronger as ℓ decreases and we tentatively ascribe them to resonances located at the interfaces air/YIG and YIG/substrate (other possibilities are flaws in the sample disk symmetry¹¹). At this power, the shape of the main resonance is identical for both the transverse and the longitudinal

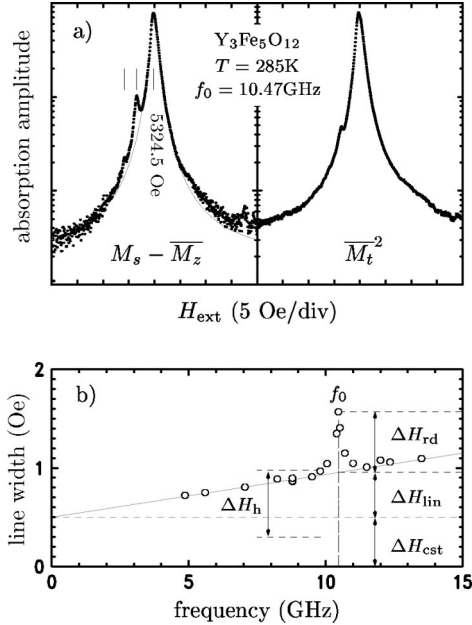


FIG. 2. (a) Line shape of the main resonance absorption line observed simultaneously along the longitudinal and transverse directions at the eigenfrequency of the microstrip resonator, 10.47 GHz. The solid line is a fit with a Lorentzian of width 1.57 Oe. (b) Frequency dependence of the linewidth measured mechanically. Contributions to the linewidth are separated between linear (ΔH_{lin}) and frequency-independent (ΔH_{cst}) relaxation channels. Homogeneous broadening (ΔH_{h}) and radiation damping effects (ΔH_{rd}) are indicated by arrows.

signals, and the main peaks can be fit with the same Lorentzian function of width $\Delta H = 1.57$ Oe.

For Lorentzian shape, the phenomenological equation of motion of the magnetic moment is the Bloch-Bloembergen form:⁶

$$\frac{d}{dt} \bar{M}_t^2 = 2 \frac{M_s P_{\text{abs}}}{H + 4\pi(n_t - n_z)M_s + H_{\text{anis}}} - 2 \frac{\bar{M}_t^2}{T_2}, \quad (1a)$$

$$\frac{d}{dt} (M_s - \bar{M}_z) = \frac{P_{\text{abs}}}{H + 4\pi(n_t - n_z)M_s + H_{\text{anis}}} - \frac{M_s - \bar{M}_z}{T_1}, \quad (1b)$$

where T_2 and T_1 denote, respectively, the transverse and longitudinal relaxation times of the magnetization. $H = H_{\text{ext}} + H_{\text{tip}}$ is the applied magnetic field (not including that of the sample), defined as the superposition of the uniform external field and stray field of the tip along z , H_{anis} is the magneto-crystalline anisotropy field, (n_t, n_z) are the depolarization factors, respectively, transverse and longitudinal, and $P_{\text{abs}} = \omega_0 \int_{V_s} dV M_y(r) H_1$ expresses the power absorbed inside the sample volume V_s . In the following, the transverse component of H_{tip} (nul at the center) is neglected. Although this formalism gives a simple relationship between the transverse relaxation rate and the homogeneous linewidth $\Delta H_h = 2/(\gamma T_2)$, it does not include inhomogeneous broadening nor does it distinguish between the different relaxation channels. Other experiments are then necessary to separate these contributions.

Further information can be obtained by performing the same measurement at different frequencies [Fig. 2(b)]. For such a small sample, the transverse signal cannot be detected if the microwave resonant circuit is detuned, hereof we have used the mechanical signal to measure the linewidth between 5 and 13.5 GHz. Three separate contributions are extracted from the data shown in Fig. 2(b). First, there is an additional broadening $\Delta H_{\text{rd}} = 0.62$ Oe at 10.47 GHz, the eigenfrequency of the microstrip resonator. It is assigned to radiation damping. In narrow linewidth materials, one should consider the feedback of the sample susceptibility on the characteristics of the microstrip resonator. It results in a diminution of the microwave amplitude H_1 around the Larmor resonance. The coupling depends on both the quality factor $Q_L \approx 150$ and the filling factor $\eta = \mathcal{O}(10^{-6})$ of the microwave circuit. The effect is thus negligible for all, but the measurements made with a tuned circuit. The second salient contribution is the linear frequency dependence of the linewidth, with a slope $\Delta H_{\text{lin}}/f = 0.043$ Oe/GHz. In single-crystals of YIG, ΔH_{lin} can be fairly well understood¹² as the sum of Kasuya-LeCraw mechanism¹³ (which accounts for ≈ 0.02 Oe/GHz) and scattering on trace amounts of rare-earth impurities. The slope is “loosely” referred to as the Gilbert coefficient, because of its viscous character ($\propto \partial M / \partial t$). This method of evaluating T_1 over a broad frequency range is limited to cases where the Gilbert coefficient is independent of the microwave frequency¹² and the orientation of M is parallel to H_{ext} .¹⁴ Finally, the third feature is a frequency-independent

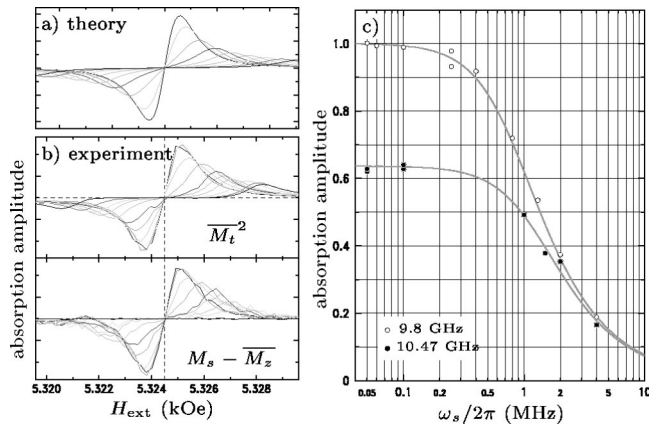


FIG. 3. Theoretical (a) and experimental (b) distortions of the anharmonic absorption line (longitudinal and transverse) for different modulation frequencies between 0.1 and 10 MHz in steps of 1 MHz. The amplitude of the frequency modulation corresponds to 10% of the linewidth. (c) Diminution of the absorption amplitude with increasing modulation frequency. The width of the 9.8 GHz bell curve gives the transverse relaxation time, $T_2 = 162$ ns. The 10.47 GHz data are normalized to the width to illustrate the effects of radiation damping.

term $\Delta H_{\text{cst}} = 0.50$ Oe which might be due to inhomogeneous broadening (like distortion in the disk shape symmetry) or scattering inside the magnon manifold (spin-spin processes). The later channel is usually associated with surface roughness or pits that couple the uniform precession to other degenerate spin waves.

Separation between homogeneous and inhomogeneous broadenings can be obtained by performing new experiments in which the amplitudes of the longitudinal and transverse components of the magnetization are independently observed for various modulation frequencies around $1/T_2$ [see Fig. 3(b)]. In this fashion, Flechter *et al.*⁷ could extract the relaxation time of all processes other than via the degenerate magnon manifold. Our longitudinal probe uses a narrow band detector limited to the audio frequency range ($\omega_c/2\pi \approx 3$ kHz). We propose to use a scheme inspired by anharmonic modulation experiments.¹⁵ The hf amplitude is fully modulated at an arbitrary frequency ω_s , while the synthesizer is frequency modulated at $\omega_f = \omega_s + \omega_c$. It should be noted that the later approach is equivalent to a modulation of the polarization field. It provides, however, a broader frequency bandwidth compared to a coil technique.

Figure 3(c) shows the result for both the transverse and the longitudinal signals. The decrease of \bar{M}_z and \bar{M}_t with increasing modulation frequency ω_s determines the homogeneous part of the broadening ΔH_h . Concentrating first on the measurements obtained with a detuned circuit (without radiation damping), a fit of 9.8 GHz data gives $\Delta H_h = 0.7 \pm 0.05$ Oe. The same model will yield a width of 1.1 Oe with the $f = 10.47$ GHz data (with radiation damping). Reporting these numbers on Fig. 2(b), the individual contributions of the 1.57 Oe linewidth observed at 10.47 GHz in Fig. 2(a) can now be detailed. First, the extrinsic contributions to the broadening contain 0.3 Oe (Ref. 16) from inhomogeneous broadening and 0.62 Oe from radiation damping. The

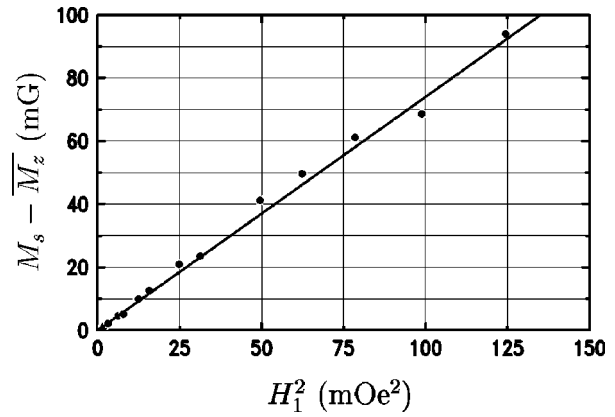


FIG. 4. Power dependence of the longitudinal component of the magnetization. The solid line is a linear fit through the data points with the slope $(M_s - \bar{M}_z)/H_1^2 \approx 740 \text{ Oe}^{-1}$.

amplitude of the radiation damping is of the same magnitude as ΔH_h , which suggests that $4\pi Q_L \eta \chi'' \approx 1$.¹⁷ The surface pits scattering accounts for 0.2 Oe, which corresponds to a spin-spin relaxation time of $T_s = 570$ ns. The result is in agreement with Hurben and Patton¹⁴ calculation of the two-magnons contribution for a normally magnetized disk of finite aspect ratio. The contribution is small because the resonance frequency of the main mode lies at the lowest point of the spin-wave spectrum so that the degenerate manifold has shrunk to almost a point.¹² Finally, the intrinsic contribution, inferred from the frequency-dependence data, is $\Delta H_{\text{lin}}|_{10.47 \text{ GHz}} = 0.45$ Oe ($1/\gamma \Delta H_{\text{lin}} = 126$ ns), which consists of Kasuya-LeCraw mechanism and relaxation from impurities.

To assess T_1 directly, we propose to use our quantitative measurements of \bar{M}_z , the spatial average of the longitudinal magnetization. At resonance,

$$T_1 P_{\text{abs}} = \int_{V_s} dV \{M_s - M_z(r)\} \{H(r) - 4\pi n_z(r) M_s\}, \quad (2)$$

which can be interpreted by saying that the energy, which is transferred to the lattice in the time T_1 , is equal to the diminution of magnetic energy stored in the sample. The important point is that it affords a direct method of measuring the spin-lattice relaxation rate at a fixed frequency. For a small precession angle, $\theta \ll 1$, the above formula can be rewritten in the more readily form $T_1 \approx (M_s - \bar{M}_z)/(\gamma^2 H_1^2 T_2 M_s)$. The transverse relaxation rate can be inferred from the homogeneous broadening $\Delta H_h = 0.7$ Oe measured at 9.8 GHz. It yields a $T_2 = 2/(\gamma \Delta H_h) = 162 \pm 10$ ns. We have plotted in Fig. 4 the measurements of the longitudinal magnetization as a function of the hf power. Using a linear fit through the data, we calculate $T_1 = 106 \pm 10$ ns,⁸ in agreement with our former evaluation of ΔH_{lin} . The value is approximately equal to $T_2/2$ which confirms that, for our geometry, the energy flows directly into lattice motions and the decay into nonuniform magnetic modes is small. Taking into account the frequency

dependence of T_1 , the obtained result compares well with the $T_1 = 137$ ns measured by Flechter *et al.*⁷ at 6.2 GHz, but part of this agreement is somewhat coincidental since it depends on the sample quality.

In conclusion, this paper describes how magnetic resonance force microscopy can be applied to the measurement of T_1 and T_2 in ferromagnetic thin films. Another important test is the detection of the Suhl second-order instability,⁴ but we find that the premature saturation of the transverse mag-

netization occurs at a lower microwave power than the predicted threshold. These results will be discussed in an upcoming paper.

We are greatly indebted to O. Acher, J. Ben Youssef, M. Goldman, and H. Le Gall for their help and support. This research was partially supported by the E.U. project M²EMS (Project No. IST-2001-34594) and the Action Concertée Nanoscience NN085.

*Electronic address: oklein@cea.fr

¹T.L. Gilbert, Phys. Rev. **100**, 1243 (1955).

²The Gilbert damping coefficient is proportional to $1/T_1$ in the linear regime.

³N. Bloembergen, Phys. Rev. **78**, 572 (1950).

⁴H. Suhl, J. Phys. Chem. Solids **1**, 209 (1957).

⁵W.K. Hiebert, A. Stankiewicz, and M.R. Freeman, Phys. Rev. Lett. **79**, 1134 (1997).

⁶N. Bloembergen and S. Wang, Phys. Rev. **93**, 72 (1954).

⁷R.C. Flechter, R.C. LeCraw, and E.G. Spencer, Phys. Rev. **117**, 955 (1960).

⁸V. V. Naletov, V. Charbois, O. Klein, and C. Fermon (unpublished).

⁹V. Charbois, V.V. Naletov, J. Ben Youssef, and O. Klein, J. Appl.

Phys. **91**, 7337 (2002).

¹⁰V. Charbois, V.V. Naletov, J. Ben Youssef, and O. Klein, Appl. Phys. Lett. **80**, 4795 (2002).

¹¹J.F. Dillon, J. Appl. Phys. **31**, 1605 (1960).

¹²M. Sparks, *Ferromagnetic Relaxation Theory* (McGraw-Hill, New York, 1964).

¹³R.C. LeCraw and E.G. Spencer, J. Phys. Soc. Jpn. **17**, 401 (1962).

¹⁴M.J. Hurben and C.E. Patton, J. Appl. Phys. **83**, 4344 (1998).

¹⁵K.J. Bruland, J. Krzystek, J.L. Garbini, and J.A. Sidles, Rev. Sci. Instrum. **66**, 2853 (1995).

¹⁶We have checked that the 0.3 Oe contribution should be assigned to a misalignment of the field with the normal of the disk.

¹⁷M.S. Seehra, Rev. Sci. Instrum. **39**, 1044 (1968).